



Published in final edited form as:

Nat Neurosci. 2017 December ; 20(12): 1686–1693. doi:10.1038/s41593-017-0005-0.

Activation of planarian TRPA1 by reactive oxygen species reveals a conserved mechanism for nociception

Oscar M. Arenas¹, Emanuela E. Zaharieva¹, Alessia Para¹, Constanza Vásquez-Doorman², Christian P. Petersen², and Marco Gallio^{1,*}

¹Department of Neurobiology, Northwestern University, Evanston, Illinois, USA

²Department of Molecular Biosciences, Northwestern University, Evanston, Illinois, USA

Abstract

All animals must detect noxious stimuli to initiate protective behavior, but the evolutionary origin of nociceptive systems is not well understood. Here, we show that noxious heat and irritant chemicals elicit robust escape behaviors in the planarian *Schmidtea mediterranea*, and that the conserved ion channel TRPA1 is required for these responses. TRPA1 mutant flies (*Drosophila*) are also defective in noxious heat responses. Unexpectedly, we find that either planarian or human TRPA1 can restore noxious heat avoidance to TRPA1 mutant *Drosophila*, even though neither is directly activated by heat. Instead, our data suggest that TRPA1 activation is mediated by H₂O₂/Reactive Oxygen Species, early markers of tissue damage rapidly produced as a result of heat exposure. Together, our data reveal a core function for TRPA1 in noxious heat transduction, demonstrate its conservation from planarians to humans, and imply that animal nociceptive systems may share a common ancestry, tracing back to a progenitor that lived more than 500 million years ago.

Introduction

Each animal group uses specialized sensory systems to detect and avoid predators, find food sources and mates. Due to specific demands, sensory systems evolve independently in different species. Yet, while each animal group lives in a sensory world that is essentially

Users may view, print, copy, and download text and data-mine the content in such documents, for the purposes of academic research, subject always to the full Conditions of use: http://www.nature.com/authors/editorial_policies/license.html#termsReprints and permissions information is available at www.nature.com/reprints.

*Correspondence and requests for materials should be addressed to M.G. (marco.gallio@northwestern.edu).

Supplementary Information **Line**

Supplementary information is linked to the on-line version of the paper at www.nature.com

Accession codes:

GeneBank: MF818036

Author contributions

M.G. designed the study, analyzed the data, and wrote the paper with critical input from all authors; O.M.A. performed all planarian behavioral experiments and electrophysiology and analyzed the corresponding data. E.E.Z. performed all fly rescue experiments and ROS assays and analyzed the corresponding data. A.P. cloned *Smed-TRPA1*, produced rescue constructs and transgenics and analyzed sequences with help from C.P.P.; A.P. O.M.A. and C.V.D. performed Q-PCR and ISH experiments. E.E.Z. and O.M.A. generated human-TRPA1 expressing flies.

The authors declare no competing financial interests.

unique, most of what we know about sensory representation comes from a very limited number of species - a handful of vertebrate and invertebrate model systems.

The detection of potentially harmful conditions is a core sensory task. The ion channel TRPA1 is remarkably conserved across animal evolution and has been implicated in the response to a broad range of electrophilic irritant chemicals as well as to noxious hot or cold temperature in humans¹, mice²⁻⁸, and flies^{2,9,10}. Interestingly, while TRPA1's sensitivity to irritant chemicals has been widely conserved (¹¹, in all but the *C. elegans* homolog¹²), its temperature gating appears to have changed repeatedly during evolution¹³. *In vitro*, some mammalian TRPA1 homologs are activated by noxious cold¹⁴, while others are insensitive to temperature (reviewed in¹³). In contrast, TRPA1 from chicken¹⁵, various reptiles, and *Xenopus* frogs are activated by warm temperatures^{16,17}, and the zebrafish genome encodes two distinct paralogs, only one of which shows thermosensory responses^{18,19}. The situation in invertebrates is also complex: while *C. elegans* TRPA1 is activated by cold¹², insect TRPA1s (honeybee²⁰, mosquito²¹ etc.) are activated by warm temperatures, and the fruit fly homolog is spliced into at least four variants¹⁰, including both heat-sensitive and heat-insensitive ones^{2,10,22}.

What is the ancestral function of TRPA1? How ancient is its association with nociceptors? Planarian flatworms are an attractive system in which to study evolutionary origins of sensory transduction. As members of the phylum Platyhelminths, planarians are considered among the simplest animals with bilateral symmetry and a centralized nervous system. From an evolutionary perspective, they are very distant from taxa that include species extensively studied such as nematodes, flies and mice (²³ and Figure 1a). Furthermore, recent work on regeneration has led to the development of RNAi protocols to systemically knock-down the expression of selected genes *in vivo*²⁴. Here, we use these tools to investigate the function of TRPA1 in the freshwater planarian *Schmidtea mediterranea*.

Results

***Schmidtea mediterranea* TRPA1 mediates noxious heat avoidance**

A fragment of the *S. mediterranea* TRPA1 gene has been previously used in *in situ* hybridization experiments as a marker for a subset of differentiated neurons²⁵. Starting from it, we cloned a full-length coding sequence for the gene (see Methods for details), henceforth referred to as *Smed-TRPA1* (Figure 1b). To test whether *Smed-TRPA1* mediates the avoidance of noxious heat in *S. mediterranea*, we designed a two-choice avoidance assay (Supplementary Figure 1) based on the one we previously developed for fruit flies²⁶. Animals were introduced into a small circular chamber covered by a thin film of water, and tracked while making a choice between floor tiles kept at moderate (24°C) or hot (32°C) temperatures; the time spent in each quadrant was then quantified to calculate an avoidance index (AI). In this assay, *S. mediterranea* showed robust avoidance of heat (32°C, AI~1), manifested as sharp turns away from the hot quadrants (Figure 1c). This is consistent with a nocifensive behavior, and indeed with the fact that *S. mediterranea* comes from cool water environments and can die from brief exposure to 35°C (²⁷ and data not shown).

Remarkably, the avoidance of hot quadrants was severely disrupted by RNAi knock-down of *Smed-TRPA1* (Figure 1c–d and see Supplementary Video 1). *Smed-TRPA1* RNAi animals glided around the chamber without turning at the hot-cold boundaries (see tracks in Figure 1c), and ended up spending nearly equal time in hot as in cool quadrants. This is in sharp contrast with the behavior of both untreated and control worms (i.e. worms fed dsRNA targeted to a sequence not present in the worm genome, Figure 1c–d). Importantly, *Smed-TRPA1* RNAi worms glided around the chamber at comparable speed as controls (Figure 1e), and displayed robust negative phototaxis when given a choice between light and dark (in an independent assay, see Supplementary Figure 2), indicating that *Smed-TRPA1* RNAi does not mar gross locomotor functions, nor does it impact all aversive behavior.

RNAi knock-down of the transcription factor AP2 has been previously shown to impair the expression of TRPA1 in *S. mediterranea*²⁵. Based on this, we reasoned that *ap2* RNAi could provide an independent means to assess the role of TRPA1 in heat nociception. Unexpectedly, *ap2* RNAi animals did not display an avoidance defect, and instead avoided the hot quadrants as robustly as controls (Figure 1c–d). *In situ* hybridization revealed that *ap2* RNAi was effective in knocking-down *Smed-TRPA1* expression only within the brain, and not in peripheral neurons (Figure 1 f–k). The fact that animals with significantly reduced *Smed-TRPA1* expression within the brain behave normally suggests that *Smed-TRPA1* is required at the periphery for the detection or responses to noxious heat.

Smed-TRPA1 is also required for chemical nociception

Next, we tested *Smed-TRPA1* knock-down animals for potential defects in chemical nociception, by assaying behavioral responses to Allyl isothiocyanate (AITC). AITC is the agent responsible for the pungent taste of mustard and wasabi, and a well-known chemical agonist of TRPA1^{3,4,8}. We developed an arena consisting of circular chambers interconnected by small corridors that are not readily traversed by the worms (Figure 2a). Animals fed control dsRNA (see above) or *Smed-TRPA1* dsRNA were introduced in the first chamber in the presence of a mock agar pellet, or -alternatively- of an agar pellet laced with AITC; their behavior was then monitored for 5 minutes. Mock pellets were readily explored by untreated animals as well as by RNAi controls, which as a result remained in their vicinity. In contrast, AITC produced strong aversive responses including rapid withdrawal and abrupt turns. The worms ultimately escaped away from the chamber containing the pellet traversing the narrow corridors (Figure 2b and Supplementary Video 2). Again in sharp contrast to controls, *Smed-TRPA1* knock-down animals did not display aversive responses and instead remained in the first chamber, in the vicinity of the AITC-laced pellet (Figure 2b).

Heterologously-expressed Smed-TRPA1 responds to AITC but not heat

Our experiments show that *Smed-TRPA1* is a key mediator of both heat avoidance and chemical nociception *in vivo* in *S. mediterranea*. To begin studying the biophysical properties of the channel *in vitro*, we next performed whole cell patch-clamp electrophysiology on heterologously expressing cells. To achieve functional expression of Smed-TRPA1, we chose *Drosophila* S2 cells, a system previously used for *Drosophila* TRPA1²⁸. Our recordings show that, in S2 cells, Smed-TRPA1 was activated by AITC

(Figure 3). In contrast, the channel was not directly gated by heat (Figure 3a–d). Even when mis-expressed *in vivo*, in transgenic *Drosophila* (i.e. in all fly neurons), Smed-TRPA1 could be readily activated by AITC, but not heat (Figure 4). As a control, the *Drosophila* TRPA1-A variant¹⁰ was activated by both AITC and heat in both contexts (Figure 3c–d and Figure 4, and²⁹).

Across-phylum rescue of *Drosophila* TRPA1 mutants by distant homologs

The lack of thermal sensitivity of *Smed-TRPA1 in vitro* (vis-à-vis the effect of RNAi on noxious heat avoidance) appears puzzling. However, TRPA1 is well known to function both as a primary temperature receptor as well as a signal transduction component, i.e. *downstream* of diverse signaling events^{7,30}. Interestingly, both the heat-nociception phenotype of TRPA1 mutant fly larvae and heat-entrainment defects of adults were readily rescued by a non-heat-sensitive variant of the fly TRPA1 (TRPA1-C,^{10,31}). These observations led us to test directly the possibility that the non-heat-sensitive Smed-TRPA1 may also be able to substitute for the fly TRPA1 –i.e. to attempt across-phylum rescue of a *Drosophila* TRPA1 mutant by expression of the planarian homolog.

First, we used a rapid 2-choice assay for temperature preference²⁶ (similar to that described above), and probed the responses of wild type and TRPA1 *Drosophila* mutants to both innocuous (30°C) and noxious heat (40°C, Figure 5a). Consistent with previous reports⁹, in our assay TRPA1 mutant flies showed a clear defect in the avoidance of noxious heat (Figure 5a,c; note that residual heat avoidance is likely mediated by *GR28b.d* –a distinct molecular hot receptor³²). Much like in the larva, this nociceptive phenotype could be significantly rescued by ubiquitous expression of *TRPA1-C*, a TRPA1 variant not directly activated by heat¹⁰ (Figure 5b,c). Strikingly, a comparable amount of rescue could be achieved by ubiquitous expression of the planarian *Smed-TRPA1* (34% identical and 53% similar to the fly TRPA1 in amino-acidic sequence; Figure 5b,c), and even of a human *TRPA1* cDNA (36% and 31% identical, and 57% and 49% similar to fly and Smed-TRPA1, respectively; Figure 5b,c).

Hydrogen peroxide and reactive oxygen species as potential mediators of TRPA1 activation

The rescue of the fly phenotype by an evolutionary distant ‘heat-insensitive’ homolog such as *Smed-TRPA1*, and the human TRPA1 (activated by cold rather than heat), argues that the function of TRPA1 in heat nociception is unlikely to be fully explained by direct heat gating. Instead, a number of observations point towards early markers of tissue damage as potential mediators of TRPA1 activation during nociceptive heat responses. Hydrogen peroxide (H₂O₂), is amongst the earliest known markers of mechanical tissue damage in vertebrates³³, *Drosophila*³⁴ as well as *Planarians*³⁵. H₂O₂ is a well-known activator of mammalian and *Drosophila* TRPA1 (^{36–39}, together with additional Reactive Oxygen Species –ROS⁴⁰), and recent work suggest that responses to potentially damaging short-wavelength UV light occurs through photochemical production of H₂O₂, and requires TRPA1 in both flies^{37–39,41} and planarians⁴². Thus, if noxious heat were to cause rapid, localized, production of H₂O₂/ROS, this could provide the direct signal for TRPA1 activation that mediates nociceptive responses.

For this hypothesis to be correct, a number of conditions have to be met: (1) *SmedTRPA1* (like human and *Drosophila*) should be activated by H₂O₂; (2) *In vivo*, heat stimulation in the appropriate range should cause rapid H₂O₂/ROS production (on a timescale compatible with the animal's escape behaviors) and, (3) if indeed nociceptive heat responses are mediated by H₂O₂/ROS, an acute increase in H₂O₂/ROS levels should sensitize the animal's behavioral responses to noxious heat, and this sensitization should depend on TRPA1. Our experiments confirm each of these predictions.

First, we tested Smed-TRPA1 for potential responses to H₂O₂ *in vitro* in our cell expression system (see above). Our recordings showed that, in S2 cells, Smed-TRPA1 was indeed activated by a range of H₂O₂ concentrations (Figure 6a,b), as was the *Drosophila* counterpart TRPA1-C (Figure 6b; i.e. the 'heat insensitive' fly variant which also supported behavioral rescue in our experiment). We note that, while it is difficult to speculate on the H₂O₂/ROS concentration that TRPA1 may encounter during a heat challenge *in vivo*, secondary modifications (such as prolyl hydroxylation⁴³) have been shown to dramatically increase TRPA1 responses to H₂O₂/ROS, potentially expanding the effective sensitivity of the channel.

Next, we tested if heat stimulation in the appropriate range (i.e. in the 'noxious' range for each species) may lead to the rapid production of H₂O₂/ROS in both *Schmidtea* and *Drosophila* tissue. For this experiment, we loaded living samples with the dye 5-(and 6)-carboxy-2',7'-dichlorodihydrofluorescein diacetate (carboxy-H₂DCFDA, a widely used fluorogenic ROS marker for live cells⁴⁴), and monitored potential fluorescence changes in response to heat exposure by confocal microscopy. As previously reported, live planarian worms could be directly loaded with the dye, and displayed H₂O₂/ROS induced fluorescence at sites of physical wounding³⁵ and data not shown; and see **ED Figure 3** for additional controls). Fast H₂O₂/ROS production was also detected when the worms were submitted to rapid heating while under the microscope (i.e. by using a heating stage; $t=20>35^{\circ}\text{C}$, speed= $\sim 1^{\circ}\text{C}/4$ seconds). Consistent with the 'noxious' range for this animal (30–35°C), we observed rapid H₂O₂/ROS increases starting above 23–25°C, and culminating in widespread fluorescence around 30–35°C (Figure 6c–e). *Drosophila* tissues also displayed rapid H₂O₂/ROS increases in response to heating, but this time the increase in fluorescence started around 30°C, and culminated around 40–45°C (Figure 6f–g), consistent with the 'noxious' range for *Drosophila* (35–40°C). Importantly, in both planarians and fly tissues, we recorded fluorescence changes rapid enough to be compatible with the timescale that would be required to trigger/modulate behavioral responses: for example between two imaging frames (Figure 6d, i.e. separated by $\sim 350\text{ms}$), or after as little as one second of exposure to heat (Figure 6h).

Carboxy-H₂DCFDA is a general oxidative stress indicator, and does not discriminate amongst different reactive oxygen species. To directly test if H₂O₂ in particular may be amongst the species produced during a noxious heat challenge, we turned to the genetically encoded H₂O₂ indicator roGFP2-Orp1. This indicator couples the redox-sensitive green fluorescent protein 2 (roGFP2) with the yeast H₂O₂ sensor Orp1, allowing the measurement of changes in H₂O₂ levels in intact living animals⁴⁵. Our results show that, in transgenic

Drosophila larvae, roGFP2-Orp1 reported a significant increase in H₂O₂ upon brief (~5 seconds) exposure to noxious heat (**Figure ED4**, see legend and methods for details).

Finally, we tested the notion that –if noxious temperatures are indeed sensed at least in part through H₂O₂/ROS production- an acute, systemic increase in H₂O₂/ROS levels may sensitize the animal’s behavioral responses to heat. Here, we tested adult *Drosophila* for heat avoidance using our 2-choice assay (see above), but this time the flies’ performance in the arena was preceded by a short feeding with H₂O₂ or Paraquat (a potent pro-oxidant⁴⁶). Strikingly, pro-oxidant feeding significantly increased heat avoidance scores in both wild type and control flies (to both 30° and 35°C) but not in TRPA1 mutant flies (Figure 6i). This result directly demonstrates that H₂O₂/ROS can sensitize aversive responses to heat in *Drosophila*, and that this sensitization requires functional TRPA1 channels.

Is TRPA1 also involved in mechanical nociception in *Schmidtea*, as it is in flies¹⁰ and mice⁴⁷? In planarians (as well as in vertebrates³³, and *Drosophila*³⁴) H₂O₂ is produced at the site of wounding³⁵ -therefore our results predict that TRPA1 signaling should also be activated by mechanical injury in *Schmidtea*. Immediately following physical damage (i.e. when cut), planarian worms engage in a behavior called “scrunching”⁴⁸, an unusual escape gait that persist for ~15 seconds after the immediate injury. Indeed, “scrunching” following physical injury was reduced in planarians in which *Smed-TRPA1* was knocked-down by RNAi (**ED Figure 5**). This result supports the notion that *Smed-TRPA1* may also be involved in mechanical nociception, and suggests a model in which either thermal or mechanical injury can activate *Smed-TRPA1* through H₂O₂/ROS production.

Discussion

Planarian flatworms are a powerful, and yet underutilized model for behavioral research. They are capable of active hunting behavior, and possess simple sensory systems^{27,49} and a simple brain that operates using synaptic and neurotransmitter principles similar to those of the more complex insect or mammalian brains⁵⁰.

Here, we have shown that the ion channel TRPA1 functions as a key transduction component for nociceptive signals in *Schmidtea mediterranea*. In insects and many vertebrates (snakes, frogs etc.), TRPA1 channels can be directly gated by temperature changes, but our work in *Schmidtea* and *Drosophila* suggests that TRPA1’s function in nociceptive heat sensing goes beyond that of a canonical heat-activated ion channel. Instead, our data suggest that H₂O₂/ROS are rapidly produced in response to noxious heat, and that this signal contributes to channel activation to mediate defensive responses. We note that this mechanism provides an especially satisfactory explanation for the remarkable across-phylum rescue of heat-avoidance phenotypes of TRPA1 mutant *Drosophila* by both *Schmidtea* TRPA1 (insensitive to heat), as well as human TRPA1 (activated by cold). The heat range that is expected to produce tissue damage in *Drosophila* (i.e. the “noxious range”, ~35–40°C) is different from that of *Schmidtea* (~30°C) from that of human (~45°C) -and yet transgenic rescue of fly mutants restored heat avoidance to that of the host (*Drosophila*) rather than the channel donor (*Schmidtea* or human). This can be accounted for by the fact that the thermal range

that causes heat damage (and therefore H₂O₂/ROS production) is determined by the heat tolerance of the host tissue.

Finally, our results suggest that early Bilaterians already possessed a polymodal (thermal/mechanical/chemical) nociceptive system that relied on H₂O₂/ROS-mediated TRPA1 activation. This core function has been conserved in extant lineages, and may have placed TRPA1 in a key position to undergo the additional transitions into a hot- or cold-activated channel that have been documented in different animal groups. Our results also imply that human pain systems may share a common ancestry with the nociceptive systems of extant bilateral animals, tracing back their origin to the common ‘Urbilaterian’ progenitor that lived more than 500 million years ago.

Methods

Cloning of a *Smed-TRPA1* full length coding sequence

A full-length *Smed-TRPA1* coding sequence was amplified by PCR starting from a *Schmidtea mediterranea* cDNA library. The library was generated by Superscript III reverse transcription (Life Technologies) from total RNA, purified from whole animals using Trizol followed by DNase treatment with DNA-free (Ambion/ThermoFisher). The following primers were used for PCR: FWD 5'-CAaaacATGAATAAAATTTCTAAAAACCGAAAAACCTC-3' and REV 5'-TTAAAAATTGTTATCTGGTTTGACAGATTCTG -3' (Kozak sequence for *Drosophila* in lower case letters). Analysis of 5' - and 3' -RACE libraries produced with SMARTer® RACE 5'/3' Kit (Clontech) confirmed that the identified sequence includes the appropriate ATG and stop codons and represents a single, full-length *Smed-TRPA1* coding sequence (3510 bp). Analysis of available RNAseq data (*SmedGD*, <http://smedgd.neuro.utah.edu/>; see Robb et al., *Genesis*. 2015 Aug;53(8):535-46) indicates that *Smed-TRPA1* likely produces a single transcript, encoding a protein of 1169 amino acids, which contains 14 N-terminal ankyrin repeats (Interpro database entry: IPR002110) followed by an ion transporter domain (Interpro database entry: IPR005821).

Phylogenetic analysis of TRPA1 homologs

A neighbor-joining phylogenetic tree was constructed using the full sequence of *bona fide* (experimentally validated) TRPA1 proteins from 24 organisms: *A. gambiae* (ACC86138), *A. aegypti* (AAEL009419), *D. melanogaster* (AEU17952), *B. mori* (NP_001296525), *C. elegans* (ABQ15208), *C. brevicauda* (AEL30802), *C. porcellus* (NP_001185699), *C. hortulanus* (ADD82932), *C. atrox* (ADD82930), *D. rerio* (NP_001007066 and NP_001007067), *D. rotundus* (AEL30803), *G. gallus* (NP_001305389), *H. armigera* (AHV83756), *H. sapiens* (NP_015628), *M. mulatta* (XP_001083172), *M. musculus* (NP_808449), *P. obsoletus lindheimeri* (ADD82929), *P. jerdonii* (AEW26660), *P. regius* (ADD82928), *R. norvegicus* (NP_997491), *T. rubripes* (XP_003968031), *T. castaneum* (LOC658860), *V. destructor* (BAO73033 and BAO73034), *X. tropicalis* (BAM42680).

Planarian RNAi

The CIW4 asexual laboratory strain of *Schmidtea mediterranea* was used for all experiments. Animals were kept in plastic containers filled with 1× artificial planarian water (APW) that contained: 1.6mM NaCl, 1mM CaCl₂, 1mM MgSO₄, 0.1mM MgCl₂, 0.1mM KCl, 1.2mM NaHCO₃. Planarians were fed with homogenized calf liver for stock maintenance. The containers were cleaned two days after feeding or once a week if starved. Templates for RNA synthesis were generated by PCR from pGEM-t vectors (Promega) harboring 1.5kb fragments of Smed-TRPA1 or Smed-AP2 cDNA; a 0.8kb UNC22 PCR product was used to generate UNC22 template as an RNAi control (UNC22 is a *C. elegans* gene not present in the *S. mediterranea* genome). The T7 RNA polymerase promoter was introduced to the 5' end or 3' end of the corresponding fragment, and 2 subsequent PCR reactions were performed to generate sense and antisense RNA strands. Sense and antisense strands were pooled together, purified by phenol-chloroform extraction, and resuspended in 16µl of water before being annealed by incubating at 72°C then 37°C and finally on ice. dsRNA was mixed with 80µl of homogenized calf liver and 2µl of red food coloring to assess food intake. Planarians were starved for at least a week and then fed the dsRNA every other day 3–4 times (15µl of food for 10–15 animals). Animals that did not feed were discarded. For behavioral experiments animals were used between one day and four days after last feeding, phototaxis was used at the end of each experiment to ensure viability.

Expression analysis by Q-PCR

Total RNA from UNC22, Smed-AP2 and Smed-TRPA1 knockdown planarians was purified using Trizol reagent (Life Technologies). First strand cDNA was synthesized using MultiScribe Reverse Transcriptase (Fisher Scientific) from DNase-treated (TURBO DNase, Ambion) total RNA. qPCR reactions were performed using the EvaGreen dye (Biotium). 4 biological replicates were run for each treatment, with clathrin mRNA detected as reference gene for quantifying expression changes using the delta-delta Ct method and normalizing to the expression obtained in the control RNAi treatment. *Smed-TRPA1* was detected using the primers 5'-ACTCTCATCAACAGACAGACTTGT-3' and 5'-ATTCAGCCTCTGGATCCATTTC-3' and *clathrin* primers were 5'-GACTGCGGGCTTCTATTGAG-3' and 5'-GCGGCAATTCTTCTGAACTC-3'. Results were compared using Kruskal-Wallis.

Fluorescent *in situ* hybridization (FISH)

Smed-TRPA1 riboprobes were generated from a PCR fragment flanked by T7 promoter sequences using RNA DIG-labeling mix (Sigma-Aldrich). After *in vitro* transcription, antisense probes were precipitated with 100% ethanol and resuspended in 25µL of deionized formamide. Planarians were killed in 5% N-Acetyl cysteine, fixed in 4% formaldehyde, followed by dehydration and overnight bleaching in 6% H₂O₂ on a light box. Animals were preserved in 100% methanol and stored at -20°C. For FISH, planarians were re-hydrated with a methanol:PBST (PBS, 0.1% triton X-100) dilution series; next, animals were treated with 10mg/ml proteinase K, post-fixed in 4% formaldehyde, and incubated at 56°C for 2 hours in pre-hybridization solution (50% of de-ionized formamide, 5× SSC, 0.1 mg/ml yeast RNA, 1% Tween-20 in DEPC-treated water). Hybridization with riboprobes was conducted

for 16h in hybridization solution (same as pre-hybridization solution plus 5% dextran sulfate). Then animals were washed in pre-hybridization solution, and then subjected to a dilution series of 2× SSC, then 0.2× SSC, and finally TNTx (0.1 M Tris pH 7.5, 0.15 M NaCl, 0.3% Triton X-100). Animals were blocked in TNTx plus 5% horse serum and 5% Western Blocking Reagent (Sigma-Aldrich) for 2h at RT, and then labeled with a sheep anti-DIG-POD antibody (1:2000, Sigma-Aldrich #11207733910) in blocking solution overnight at 4°C. Animals were washed 8X in TNTx, incubated in Tyramide solution with rhodamine (1:500) and H₂O₂ for 10 minutes with shaking. Finally, animals were rinsed 6X in TNTx. ISH experiments were performed four times with similar results. To quantify TRPA1+ cells in various groups (Figure 1F–K), ten worms per treatment were imaged with a Leica DM 2500 confocal microscope with a 10× objective and 1.5 digital zoom, and Z-stacks encompassing the thickness of each animal were acquired at 5 μm intervals, using constant laser and PMT settings. Z-stacks were analyzed using ImageJ: Brightness/Contrast was adjusted in batch using identical settings and max projection images through the animal were produced. From these, the number of fluorescent cells in a defined ROI in the brain region and a defined ROI at the periphery (each of constant size, shown as yellow boxes in Figure 1) were counted. The number of fluorescent cells was then plotted and compared by unpaired t-test.

Planarian behavioral assays: heat avoidance

Heat avoidance was measured in the “Planariometer” (see Supplementary Figure 1). The Planariometer consisted in four independent tiles covered by thin anodized aluminum foil. A hydrophobic ink pen (Super PAP pen – ThermoFisher) was used to create a circular barrier (55mm of diameter) to allow a thin film of water (1–2 mm) to form a central pool in which the worms can move freely. In each experiment, 2 opposite tiles were set at 32°C and 2 at 24°C and animal movement was recorded for 4 minutes. The spatial configuration of hot and cool tiles was then reversed for 4 additional minutes (and a second movie acquired) to control for potential spatial biases. Experiments were conducted in the dark with infrared (IR) LED illumination and videos were recorded with an IR-sensitive CCD camera (Basler). Five independent groups of 10 animals per treatment were used. The heat avoidance index (AI = #worms at 24°C - #worms at 32°C/total #worms) was calculated from the last 120 frames of each video (last minute of the video) by measuring the positions of the worms every 3 frames using standard Matlab scripts. Avoidance index values were compared using Kruskal–Wallis followed by Tukey's honest significant difference test.

Planarian behavioral assays: AITC avoidance

Five independent groups of 10 animals per treatment were tested in an arena composed of two circular chambers connected by a narrow corridor. At the beginning of the experiment, all animals were placed in chamber 1 together with a small block of control agar (1% agarose dissolved in 1× APW) or AITC laced agar. The AITC laced agar was made with 1% agarose in 1× APW and 50mM AITC. The chamber was placed in the dark, animals were illuminated with IR light and their behavior was recorded for 5 minutes with an IR-sensitive CCD camera. Videos were analyzed and the number of planarians in each chamber was quantified every 10 frames for the last 125 frames of the video (last minute). The fraction of animals in each chamber was counted after each treatment and compared using Kruskal–

Wallis followed by Tukey's honest significant difference test. Image analysis was performed using Matlab.

Planarian behavioral assays: Negative phototaxis

Four independent groups of 10 worms per treatment were placed in chamber 1 of the arena as described above (AITC avoidance experiments). The arena was either kept completely dark (control condition), alternatively, chamber 1 was exposed to bright light while chamber 2 was kept dark. Animals were allowed to distribute for 2 minutes before the number of worms in each chamber was counted.

Planarian behavioral assays: scrunching

Scrunching behavior was assessed as previously described in⁴⁸, with modifications. Animals were recorded under a standard dissecting scope equipped with a Pointgrey USB camera. Planarians were placed on a wet filter paper and the tail was amputated with a scalpel while recording. Amputation was set as time=0 and total body area was subsequently measured 3 times per second for 15 seconds. Area measurements were normalized to the mean body area for each animal, averaged across the movie. Average wave amplitude was calculated across the 15' movie and compared using unpaired t-tests. Image analysis was performed using Matlab.

Cell transfections

pAC-GFP, pAC-Smed-TRPA1 and pAC-dTRPA1-A were generated by cloning GFP, *Smed-TRPA1* ORF (see above) and a dTRPA1-A cDNA (a gift of Dan Tracey) into pCRTM8/GW/TOPO® TA (ThermoFisher) and then transferring them into pAC-GW expression vector [created by ligating the Gateway cassette from pMartini Gate C R2-R1 (Addgene plasmid #36436) cut with XhoI and XbaI into pAc5.1/V5-His A (ThermoFisher)]. S2R+ cells (a gift from R. Carthew) were cultured in Schneider's Drosophila Medium (Lonza) supplemented with 10% fetal bovine serum and 1% penicillin-Streptomycin mixture (100units/mL and 100µg/mL respectively, Fisher Scientific). For electrophysiological recordings, S2R+ cells were grown on coverslips in Schneider's Drosophila Medium supplemented with 50µM LaCl₃ and transfected with 50ng of pAC-GFP vector and 500ng of either pAC-dTRPA1-A or pAC-Smed-TRPA1 vectors mixed with 4µl of enhancer and 150µl of buffer EC. After 5 min, 6.5µl of Effectene® Transfection Reagent (Qiagen) was added and the mix was incubated for 10min before being dispensed to the cells. Transfected cells were incubated at RT for at least 36h to allow gene expression.

Electrophysiological recordings

Whole cell voltage clamp was performed on S2R+ transfected cells identified by GFP fluorescence. The intracellular solution contained: 140mM methanesulfonic acid, 2mM MgCl₂, 1mM EGTA, 5 mM HEPES, 1mM Na₂ATP; pH was adjusted to 7.3 with CsOH and the osmolarity was adjusted to 315 ± 5mOsm with sucrose. The extracellular solution contained: 140mM NaCl, 5mM KCl, 1mM CaCl₂, 1mM HEPES, 10mM Glucose; pH was adjusted to 7.2 with NaOH and the osmolarity was adjusted to 310 ± 5 mOsm with sucrose. Patch pipettes resistance ranged from 5 to 10MΩ. Recordings were obtained with an

AxoPatch 200b amplifier (Axon Instruments), and analyzed with AxoGraph software and Matlab scripts. Recordings were made with $1\times$ output gain and 5KHz low pass filter. Bath offset and capacitance were compensated; series resistance was $9.5\pm 5.5M\Omega$ without compensation. Recordings were made at RT (22–23°C) and temperature stimulation was achieved by raising the temperature of the bath solution via an inline heater (HPT-2A, ALA Scientific Instruments) and a TC-20 temperature controller (NPI Electronics). Temperature was monitored with a T-384 thermocouple (Physitemp Instruments) tethered to the electrode holder, so that the tip of the thermocouple was approximately at a constant distance from the tip of the recording electrode (1–2 mm). Chemical stimulation was achieved by bath perfusion of extracellular solution containing 500 μ M of allyl isothiocyanate (AITC, Sigma). Cells were held at -60 mV and currents were monitored during heat and chemical stimulation. Current-voltage relationships were constructed by averaging three step protocols consisting of 100ms steps of 20mV from -100 to 100mV separated by 400ms. These IV relationships were made at RT, during the heat stimulation, and at the end of a 3min AITC application. Note that *Smed-TRPA1* did not appear to respond to cooling. For the AITC and Hydrogen peroxide dose responses (H_2O_2 , Sigma, 30% w/w) we used 1 min stimulation at each concentration. Recordings were performed as described above with the exception that the intracellular solution contained 140mM K-gluconate instead of Cesium.

Fly strains and transgenes

Flies were reared on standard cornmeal agar medium at room temperature (RT). The following fly strains were used: Canton-special, isogenic w^{1118} (a gift from Marcus C. Stensmyr); *elav-Gal4/CyO*; *trpA1¹* (BDSC#26504, backcrossed 5 times); 5xUAS-TRPA1-C (a gift from D. Tracey); *tub-cyto-roGFP2-Orp1⁴⁹*. To generate *UAS-SmedTRPA1* flies, *Smed-TRPA1* cDNA (see above) was cloned into pCRTM8/GW/TOPO[®] TA (Invitrogen) and then transferred into a 40xUAS destination vector created introducing the Gateway[®] cassette into pJFRC8-40XUAS- IVS-mCD8::GFP (Addgene #26221) via the XhoI/ XbaI restriction sites. This construct was then used for embryo injection by BestGene Inc. to generate P[40XUAS::Smed-TRPA1]attP40 flies. Similarly, *UAS-humanTRPA1* flies were obtained starting from a human TRPA1 cDNA (NP_015628; a gift from Mark Hoon) to generate P[40XUAS::hTRPA1]attP40 flies. Expression of the transgenes was confirmed by RT PCR. Full genotypes of fly stocks used in Figure 5: w^{1118} . w^{1118} ; *TRPA1¹*. w^{1118} ; *elav-Gal4/+*; *TRPA1¹/TRPA1¹*. w^{1118} ; *+UAS-TRPA1-C*; *TRPA1¹/TRPA1¹*. w^{1118} ; *elav-Gal4/UAS-TRPA1-C*; *TRPA1¹/TRPA1¹*. w^{1118} ; *+UAS-Smed-TRPA1*; *TRPA1¹/TRPA1¹*. w^{1118} ; *elav-Gal4/UAS-Smed-TRPA1*; *TRPA1¹/TRPA1¹*. w^{1118} ; *+UAS-human TRPA1*; *TRPA1¹/TRPA1¹*. w^{1118} ; *elav-Gal4/UAS-human TRPA1*; *TRPA1¹/TRPA1¹*.

Drosophila behavioral assays

Temperature preference assay were performed as previously described (Gallio et al., 2011). In brief, Avoidance Index (AI) values for the test temperatures (TT) are calculated as follows: $AI = \frac{\# \text{flies at } 25^\circ\text{C} - \# \text{flies at TT}}{\text{total } \# \text{flies}}$. AI values were compared using ANOVA or 2-way ANOVA as previously described. Avoidance index values for experiments with Gal4 and UAS lines were compared by two-way ANOVA (threshold $P = 0.01$). Kolmogorov Smirnov tests were used to test for a normally distributed sample. Homogeneity of variance for each data set was confirmed by calculating the Spearman

correlation between the absolute values of the residual errors and the observed values of the dependent variable (threshold $P = 0.05$). Statistical analysis was carried out in MATLAB. All temperature preference experiments were performed on 3–5 days old male flies in a custom chamber kept at a constant RH of 40%. Heat and AITC-vapor incapacitation experiments (Figure 4) were performed as follows: Flies of the genotypes *elav/+*, *UAS-Smed-TRPA1/+*, *UAS-TRPA1-1/+* (negative controls), *elav-Gal4>UAS-TRPA1-A* (positive control) and *elav-Gal4>UAS-Smed-TRPA1* (experimental animals), were used to test responses to temperature and AITC. For heat incapacitation, groups of 10 flies were collected in empty vials and placed in a 25°C incubator for at least an hour before the experiments. Next, the vials were submerged in water (pre-heated to 35°C) and kept submerged until the internal air temperature of the tube had been at 35°C for one minute (as measured by a thermocouple). Following this, the number of incapacitated flies (i.e. flies that had dropped to the bottom of the tube) was counted. Vials were then placed at RT for three additional minutes, and the number of incapacitated flies scored every minute to measure recovery. For the exposure to AITC vapors, groups of 10 flies of each genotype (see above), were collected in 15mL tubes for bacterial culture with small holes to allow air flow. These 15mL culture tube were placed inside a 50mL conical tube containing a small piece of filter paper with 1µl of 2.5M AITC. Flies were exposed to AITC vapors for 10 minutes and then transferred to clean vials for recovery. The number of incapacitated animals was recorded every minute during AITC exposure and every 5 minutes during recovery. For the pro-oxidant feeding experiments, groups of twenty 3–5 day-old flies of the appropriate genotype were starved for 18 hours in vials with a Kim-wipe saturated by water. Flies were then fed for three hours on Nutri-Fly™ Instant Medium (Genesee Scientific #66–117) prepared with the respective pro-oxidant solution at a ratio of medium to liquid of 1:3. The liquid used contained the pro-oxidant and sucrose, or sucrose alone ('mock'). Final concentrations: all samples=2% sucrose; H₂O₂=5%, Paraquat (Sigma #856177)=50mM. Immediately after, the animals were tested for temperature preference as described above. Food intake was monitored in parallel experiments using green food colorant (25µl for 3ml of solution).

ROS imaging

To evaluate ROS levels in response to heat stimuli in intact live planarians and *Drosophila* tissues, we used the fluorogenic oxidative stress indicator carboxy-H2DCFDA (Molecular Probes #I36007) per the manufacturer's guidelines (and see below). ROS levels were imaged on an LSM510 Zeiss confocal microscope equipped using a 488 argon laser. Temperature stimuli were generated with a Model 5000 KT stage controller (20/20 Technology) and the temperature was recorded using NI USB-TC01 equipped with a thermocouple probe (National Instruments). Intact planarians were incubated for an hour in 25µM carboxy-H2DCFDA (diluted in APW) and washed briefly in APW prior to imaging. To minimize movements during scanning, animals were placed into a tight-fitting custom made Sylgard frame mounted on a glass slide and filled with APW. The preparation was sealed with a cover slip. For real time ROS detection, planarians were imaged continuously with a 5×/0.16 Zeiss air objective at 256×256 pixel resolution and 2× optical zoom at 0.395msec frame rate during a heat ramp of $t=20>35^{\circ}\text{C}$, speed= $\sim 1^{\circ}\text{C}/4$ seconds. ROS induced fluorescence was measured from confocal images acquired at low resolution and using a fully open pinhole,

from ROIs corresponding to large parts of the head region (512×512 pixel resolution 1× optical zoom with a 5×Zeiss air objective). *Drosophila* salivary glands were dissected in PBS and incubated with 25µM carboxy-H2DCFDA (diluted in PBS) for an hour at room temperature prior to heat stimulation. Tissues were then briefly washed in PBS and transferred into a custom made thin Sylgard frame containing PBS and mounted on a glass slide. The preparation was sealed with a cover slip. Differences in fluorescence were evaluated using unpaired t-tests. For real time ROS detection in *Drosophila*, salivary glands were imaged continuously with a 10×Zeiss air objective at 256×256 pixel resolution and 2× optical zoom at 0.395msec frame rate during a heat ramp of $t=20>45^{\circ}\text{C}$, speed= $\sim 1^{\circ}\text{C}/4$ seconds. DF/F analysis was carried out using MATLAB scripts, base fluorescence was calculated using all frames preceding temperature trigger (occurring at 30s). Confocal stacks of about 100 µm at 5 µm steps were obtained at 512×512 pixel resolution 1× optical zoom with a 10× Zeiss air objective. For in vivo H2O2 detection in intact animals, tub-cyto-roGFP2-Orp1 larvae were placed on a heated surface set to $\sim 35^{\circ}\text{C}$ for 5 seconds. As a positive control, larvae were exposed to 25 µM H2O2 for 10 minutes. Animals were rapidly dissected post treatment in PBS to extract their wing imaginal discs (as described in ref #50). The tissues were mounted in glycerol and immediately imaged on a Leica SP5 inverted confocal microscope equipped with a 405 UV and a 488 Argon laser and a 10× air objective at 512×512 pixel resolution and 400 Hz. Image acquisition and processing were performed as above. We used two-sample T-test to calculate significant difference ($p<0.05$) between treatments and controls. Excitation of the biosensor fluorescence by the 405 nm and 488 nm laser lines was performed sequentially and stack by stack. Emission was detected at 500–570 nm. Image processing was performed with imageJ. Control fluorescence (i.e. of untreated tissue) was set to 1.

Statistics

No statistical methods were used to predetermine sample size. Sample sizes were chosen following accepted standards in the field. No randomization was used. Data collection and analysis were not performed blind to the conditions of the experiments. No animals or data points were excluded from the analyses. Statistical testing was performed using Matlab. Normal data distribution was assessed by Kolmogorov-Smirnov tests. If normality was met, we used unpaired Student's t tests and two-way ANOVA for single and multiple comparisons, respectively. If normality was not met, we used Kruskal-Wallis. Data graphs were processed using the notBoxPlot Matlab function (kindly provided to the community by Rob Campell). A Supplementary Methods Checklist and a Life Sciences Reporting Summary are available on-line.

Data availability

The data that support the findings of this study are available from the corresponding author upon reasonable request.

Code availability

Our analysis uses standard Matlab functions (Image analysis and Statistics toolboxes).

Supplementary Material

Refer to Web version on PubMed Central for supplementary material.

Acknowledgments

We thank D. Tracey and R. Carthew for reagents. Andrew Kuang and Leah Vinson for technical assistance, Lindsey Macpherson, David Yarmolinsky and members of the Gallio Lab for comments on the manuscript, Indra Raman for technical advice and Marcus Stensmyr for the kind gift of the fly drawing in Fig 1. Work in the Gallio lab is supported by NIH grant R01NS086859 (to M.G.), the Chicago Biomedical Consortium with support from the Searle Funds at the Chicago Community Trust (to E.E.Z.), and by training grant 2T32MH067564 (to O.M.A.). Work in the Petersen Lab is supported by an NIH Director's New Innovator award (1DP2DE024365-01).

References

1. Kremeyer B, et al. A gain-of-function mutation in TRPA1 causes familial episodic pain syndrome. *Neuron*. 2010; 66:671–680. DOI: 10.1016/j.neuron.2010.04.030 [PubMed: 20547126]
2. Viswanath V, et al. Opposite thermosensor in fruitfly and mouse. *Nature*. 2003; 423:822–823. DOI: 10.1038/423822a [PubMed: 12815418]
3. Jordt SE, et al. Mustard oils and cannabinoids excite sensory nerve fibres through the TRP channel ANKTM1. *Nature*. 2004; 427:260–265. DOI: 10.1038/nature02282 [PubMed: 14712238]
4. Bandell M, et al. Noxious cold ion channel TRPA1 is activated by pungent compounds and bradykinin. *Neuron*. 2004; 41:849–857. [PubMed: 15046718]
5. Macpherson LJ, et al. The pungency of garlic: activation of TRPA1 and TRPV1 in response to allicin. *Current biology : CB*. 2005; 15:929–934. DOI: 10.1016/j.cub.2005.04.018 [PubMed: 15916949]
6. Bautista DM, et al. Pungent products from garlic activate the sensory ion channel TRPA1. *Proceedings of the National Academy of Sciences of the United States of America*. 2005; 102:12248–12252. DOI: 10.1073/pnas.0505356102 [PubMed: 16103371]
7. Bautista DM, et al. TRPA1 Mediates the Inflammatory Actions of Environmental Irritants and Proalgesic Agents. *Cell*. 2006; 124:1269–1282. doi:<http://dx.doi.org/10.1016/j.cell.2006.02.023>. [PubMed: 16564016]
8. Macpherson LJ, et al. An ion channel essential for sensing chemical damage. *The Journal of neuroscience : the official journal of the Society for Neuroscience*. 2007; 27:11412–11415. DOI: 10.1523/JNEUROSCI.3600-07.2007 [PubMed: 17942735]
9. Neely GG, et al. TrpA1 regulates thermal nociception in *Drosophila*. *PloS one*. 2011; 6:e24343. [PubMed: 21909389]
10. Zhong L, et al. Thermosensory and nonthermosensory isoforms of *Drosophila melanogaster* TRPA1 reveal heat-sensor domains of a thermoTRP Channel. *Cell reports*. 2012; 1:43–55. DOI: 10.1016/j.celrep.2011.11.002 [PubMed: 22347718]
11. Kang K, et al. Analysis of *Drosophila* TRPA1 reveals an ancient origin for human chemical nociception. *Nature*. 2010; 464:597–600. DOI: 10.1038/nature08848 [PubMed: 20237474]
12. Chatzigeorgiou M, et al. Specific roles for DEG/ENaC and TRP channels in touch and thermosensation in *C. elegans* nociceptors. *Nature neuroscience*. 2010; 13:861–868. DOI: 10.1038/nn.2581 [PubMed: 20512132]
13. Laursen WJ, Bagriantsev SN, Gracheva EO. TRPA1 channels: chemical and temperature sensitivity. *Current topics in membranes*. 2014; 74:89–112. DOI: 10.1016/B978-0-12-800181-3.00004-X [PubMed: 25366234]
14. Chen J, et al. Species differences and molecular determinant of TRPA1 cold sensitivity. *Nature communications*. 2013; 4:2501.
15. Saito S, et al. Heat and noxious chemical sensor, chicken TRPA1, as a target of bird repellents and identification of its structural determinants by multispecies functional comparison. *Molecular biology and evolution*. 2014; 31:708–722. DOI: 10.1093/molbev/msu001 [PubMed: 24398321]

16. Gracheva EO, et al. Molecular basis of infrared detection by snakes. *Nature*. 2010; 464:1006–1011. DOI: 10.1038/nature08943 [PubMed: 20228791]
17. Saito S, et al. Analysis of transient receptor potential ankyrin 1 (TRPA1) in frogs and lizards illuminates both nociceptive heat and chemical sensitivities and coexpression with TRP vanilloid 1 (TRPV1) in ancestral vertebrates. *The Journal of biological chemistry*. 2012; 287:30743–30754. DOI: 10.1074/jbc.M112.362194 [PubMed: 22791718]
18. Oda M, Kurogi M, Kubo Y, Saitoh O. Sensitivities of Two Zebrafish TRPA1 Paralogs to Chemical and Thermal Stimuli Analyzed in Heterologous Expression Systems. *Chemical senses*. 2016; 41:261–272. DOI: 10.1093/chemse/bjv091 [PubMed: 26826723]
19. Prober DA, et al. Zebrafish TRPA1 channels are required for chemosensation but not for thermosensation or mechanosensory hair cell function. *The Journal of neuroscience : the official journal of the Society for Neuroscience*. 2008; 28:10102–10110. DOI: 10.1523/JNEUROSCI.2740-08.2008 [PubMed: 18829968]
20. Kohno K, Sokabe T, Tominaga M, Kadowaki T. Honey bee thermal/chemical sensor, AmHsTRPA, reveals neofunctionalization and loss of transient receptor potential channel genes. *The Journal of neuroscience : the official journal of the Society for Neuroscience*. 2010; 30:12219–12229. DOI: 10.1523/JNEUROSCI.2001-10.2010 [PubMed: 20844118]
21. Wang G, et al. Anopheles gambiae TRPA1 is a heat-activated channel expressed in thermosensitive sensilla of female antennae. *The European journal of neuroscience*. 2009; 30:967–974. DOI: 10.1111/j.1460-9568.2009.06901.x [PubMed: 19735290]
22. Kang K, et al. Modulation of TRPA1 thermal sensitivity enables sensory discrimination in *Drosophila*. *Nature*. 2012; 481:76–80. DOI: 10.1038/nature10715
23. Dunn CW, Giribet G, Edgecombe GD, Hejnol A. Animal Phylogeny and Its Evolutionary Implications. *Annual Review of Ecology, Evolution, and Systematics*. 2014; 45:371–395. doi: DOI: 10.1146/annurev-ecolsys-120213-091627
24. Newmark PA, Reddien PW, Cebria F, Sanchez Alvarado A. Ingestion of bacterially expressed double-stranded RNA inhibits gene expression in planarians. *Proceedings of the National Academy of Sciences of the United States of America*. 2003; 100(Suppl 1):11861–11865. DOI: 10.1073/pnas.1834205100 [PubMed: 12917490]
25. Wenemoser D, Lapan SW, Wilkinson AW, Bell GW, Reddien PW. A molecular wound response program associated with regeneration initiation in planarians. *Genes & development*. 2012; 26:988–1002. DOI: 10.1101/gad.187377.112 [PubMed: 22549959]
26. Gallio M, Ofstad TA, Macpherson LJ, Wang JW, Zuker CS. The coding of temperature in the *Drosophila* brain. *Cell*. 2011; 144:614–624. DOI: 10.1016/j.cell.2011.01.028 [PubMed: 21335241]
27. Inoue T, Yamashita T, Agata K. Thermosensory signaling by TRPM is processed by brain serotonergic neurons to produce planarian thermotaxis. *The Journal of neuroscience : the official journal of the Society for Neuroscience*. 2014; 34:15701–15714. DOI: 10.1523/JNEUROSCI.5379-13.2014 [PubMed: 25411498]
28. Wang H, Schupp M, Zurborg S, Heppenstall PA. Residues in the pore region of *Drosophila* transient receptor potential A1 dictate sensitivity to thermal stimuli. *The Journal of physiology*. 2013; 591:185–201. DOI: 10.1113/jphysiol.2012.242842 [PubMed: 23027824]
29. Cordero-Morales JF, Gracheva EO, Julius D. Cytoplasmic ankyrin repeats of transient receptor potential A1 (TRPA1) dictate sensitivity to thermal and chemical stimuli. *Proceedings of the National Academy of Sciences of the United States of America*. 2011; 108:E1184–1191. DOI: 10.1073/pnas.1114124108 [PubMed: 21930928]
30. Kwon Y, Shim H-S, Wang X, Montell C. Control of thermotactic behavior via coupling of a TRP channel to a phospholipase C signaling cascade. *Nature neuroscience*. 2008; 11:871–873. doi:http://www.nature.com/neuro/journal/v11/n8/suppinfo/nn.2170_S1.html. [PubMed: 18660806]
31. Lee Y, Montell C. *Drosophila* TRPA1 functions in temperature control of circadian rhythm in pacemaker neurons. *The Journal of neuroscience : the official journal of the Society for Neuroscience*. 2013; 33:6716–6725. DOI: 10.1523/JNEUROSCI.4237-12.2013 [PubMed: 23595730]
32. Ni L, et al. A gustatory receptor paralogue controls rapid warmth avoidance in *Drosophila*. *Nature*. 2013; 500:580–584. DOI: 10.1038/nature12390 [PubMed: 23925112]

33. Niethammer P, Grabher C, Look AT, Mitchison TJ. A tissue-scale gradient of hydrogen peroxide mediates rapid wound detection in zebrafish. *Nature*. 2009; 459:996–999. doi:http://www.nature.com/nature/journal/v459/n7249/supinfo/nature08119_S1.html. [PubMed: 19494811]
34. Moreira S, Stramer B, Evans I, Wood W, Martin P. Prioritization of Competing Damage and Developmental Signals by Migrating Macrophages in the *Drosophila* Embryo. *Current Biology*. 2010; 20:464–470. DOI: 10.1016/j.cub.2010.01.047 [PubMed: 20188558]
35. Pirotte N, et al. Reactive Oxygen Species in Planarian Regeneration: An Upstream Necessity for Correct Patterning and Brain Formation. *Oxidative medicine and cellular longevity*. 2015; 2015:392476. [PubMed: 26180588]
36. Andersson DA, Gentry C, Moss S, Bevan S. Transient receptor potential A1 is a sensory receptor for multiple products of oxidative stress. *The Journal of neuroscience : the official journal of the Society for Neuroscience*. 2008; 28:2485–2494. DOI: 10.1523/jneurosci.5369-07.2008 [PubMed: 18322093]
37. Du EJ, et al. Nucleophile sensitivity of *Drosophila* TRPA1 underlies light-induced feeding deterrence. *eLife*. 2016; 5
38. Guntur AR, et al. H₂O₂-Sensitive Isoforms of *Drosophila melanogaster* TRPA1 Act in Bitter-Sensing Gustatory Neurons to Promote Avoidance of UV During Egg-Laying. *Genetics*. 2017; 205:749–759. DOI: 10.1534/genetics.116.195172 [PubMed: 27932542]
39. Guntur AR, et al. *Drosophila* TRPA1 isoforms detect UV light via photochemical production of H₂O₂. *Proceedings of the National Academy of Sciences of the United States of America*. 2015; 112:E5753–5761. DOI: 10.1073/pnas.1514862112 [PubMed: 26443856]
40. Xu C, Luo J, He L, Montell C, Perrimon N. Oxidative stress induces stem cell proliferation via TRPA1/RyR-mediated Ca²⁺ signaling in the *Drosophila* midgut. *eLife*. 2017; 6
41. Kim MJ, Johnson WA. ROS-mediated activation of *Drosophila* larval nociceptor neurons by UVC irradiation. *BMC neuroscience*. 2014; 15:14. [PubMed: 24433322]
42. Birkholz TR, Beane WS. The planarian TRPA1 homolog mediates extraocular behavioral responses to near ultraviolet light. *The Journal of experimental biology*. 2017
43. Miyake T, et al. Cold sensitivity of TRPA1 is unveiled by the prolyl hydroxylation blockade-induced sensitization to ROS. *Nature communications*. 2016; 7:12840.
44. Kalyanaraman B, et al. Measuring reactive oxygen and nitrogen species with fluorescent probes: challenges and limitations. *Free radical biology & medicine*. 2012; 52:1–6. DOI: 10.1016/j.freeradbiomed.2011.09.030 [PubMed: 22027063]
45. Albrecht SC, Barata AG, Grosshans J, Teleman AA, Dick TP. In vivo mapping of hydrogen peroxide and oxidized glutathione reveals chemical and regional specificity of redox homeostasis. *Cell metabolism*. 2011; 14:819–829. DOI: 10.1016/j.cmet.2011.10.010 [PubMed: 22100409]
46. Rzezniczak TZ, Douglas LA, Watterson JH, Merritt TJ. Paraquat administration in *Drosophila* for use in metabolic studies of oxidative stress. *Analytical biochemistry*. 2011; 419:345–347. DOI: 10.1016/j.ab.2011.08.023 [PubMed: 21910964]
47. Kwan KY, et al. TRPA1 contributes to cold, mechanical, and chemical nociception but is not essential for hair-cell transduction. *Neuron*. 2006; 50:277–289. DOI: 10.1016/j.neuron.2006.03.042 [PubMed: 16630838]
48. Cochet-Escartin O, Mickolajczyk KJ, Collins EM. Scrunching: a novel escape gait in planarians. *Physical biology*. 2015; 12:056010. [PubMed: 26356147]
49. Inoue T, Hoshino H, Yamashita T, Shimoyama S, Agata K. Planarian shows decision-making behavior in response to multiple stimuli by integrative brain function. *Zoological letters*. 2015; 1:7. [PubMed: 26605052]
50. Umesono Y, Tasaki J, Nishimura K, Inoue T, Agata K. Regeneration in an evolutionarily primitive brain—the planarian *Dugesia japonica* model. *The European journal of neuroscience*. 2011; 34:863–869. DOI: 10.1111/j.1460-9568.2011.07819.x [PubMed: 21929621]

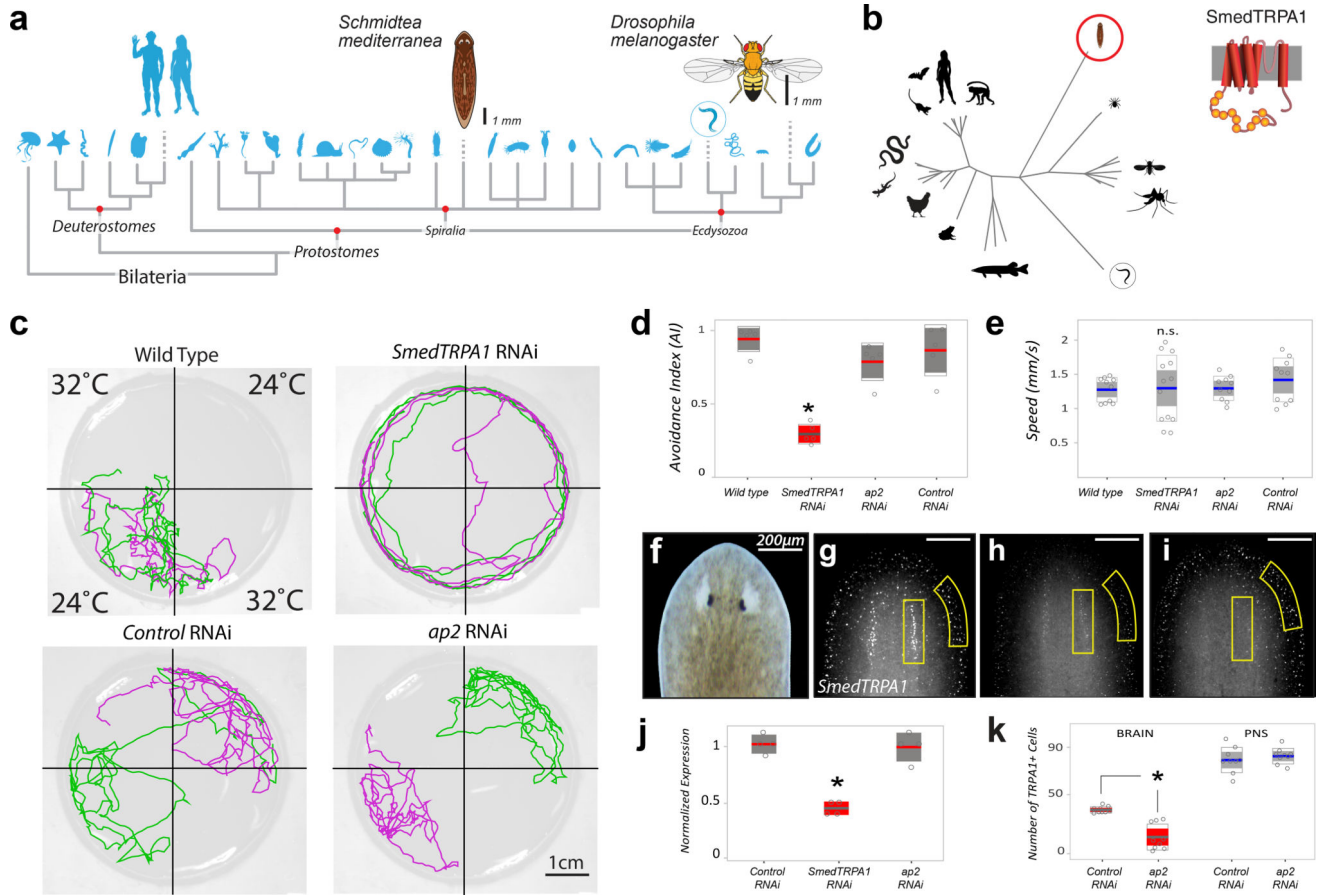


Figure 1.

Smed-TRPA1 is required for noxious heat avoidance in the planarian worm *S. mediterranea*.

a) Phylogeny of Bilateria, showing the position of *Schmidtea* (*C. elegans* is circled). **b)** Phylogenetic tree constructed from an alignment of full-length TRPA1 protein sequences from a variety of species, *Smed-TRPA1* is circled and a model of the channel's structure is shown (circles=ankyrin repeats, cylinders=transmembrane domains). **c)** 2-choice assay for heat avoidance. In each trial two opposing floor tiles are set to 24°C and two to 32°C (noxious heat). Tracks of two worms during one such trial are shown in green and purple. Unlike wild-type, controls (*unc22* RNAi), and *ap2* RNAi, *Smed-TRPA1* RNAi animals were not confined to the cool quadrants. **d)** Avoidance index for 32°C for RNAi animals. *Smed-TRPA1* RNAi animals show a reduced avoidance index for heat (N= 5 groups of 10 animals, *P= 0.0054, Kruskal-Wallis; Chi-sq(3,16)=12.68). **e)** *Smed-TRPA1* RNAi does not impact the animal's speed of movement (N=10–13 animals; n.s. = not significantly different, P= 0.6, Kruskal-Wallis; Chi-sq(3,39)=1.48). **f–i)** *In situ* hybridization with a *Smed-TRPA1* probe in **(g)** Control (*unc22* RNAi, **(h)** *Smed-TRPA1* RNAi and **(i)** *ap2* RNAi animals (head region, see **f**), demonstrates overall reduction of mRNA by *Smed-TRPA1* RNAi (independent quantification by Q-PCR is shown in **j**; N=4 replicates of 3 animals each, *P= 0.02, Kruskal-Wallis; Chi-sq(2,9)=7.65). **k)** In contrast, *ap2* RNAi reduces the number of *Smed-TRPA1*-expressing cells in the brain region, but not in the periphery (N=9 animals,

* $P = 1.5 \times 10^{-5}$; unpaired t-test, $t(16) = 6.1048$; in all plots, line=mean; outer boxes = \pm STD; inner boxes = 95% Confidence Interval.

Author Manuscript

Author Manuscript

Author Manuscript

Author Manuscript

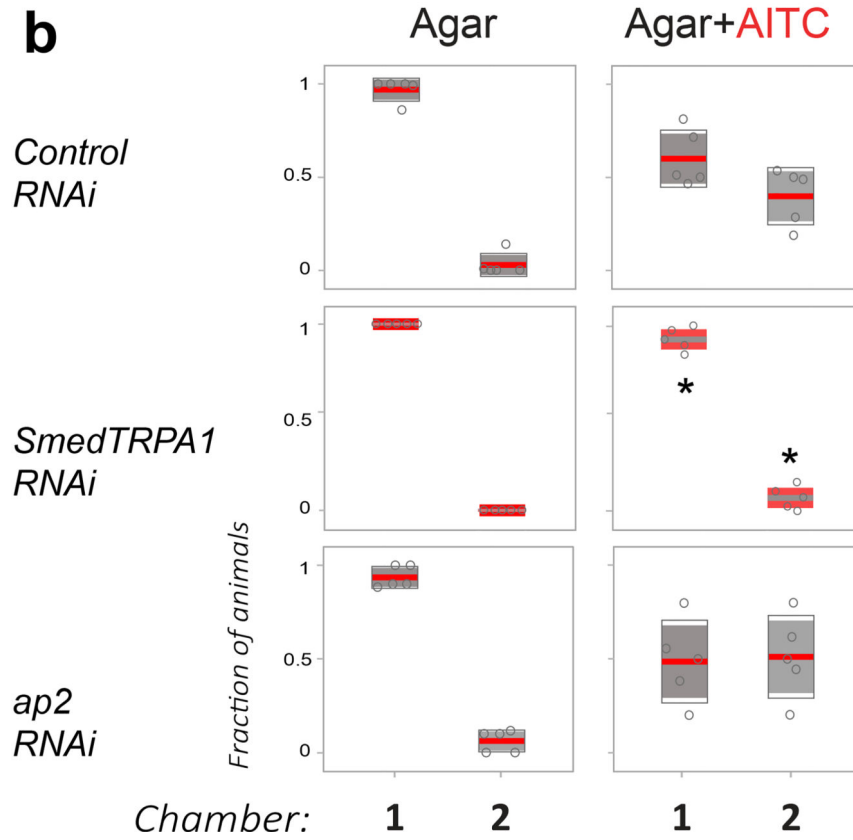
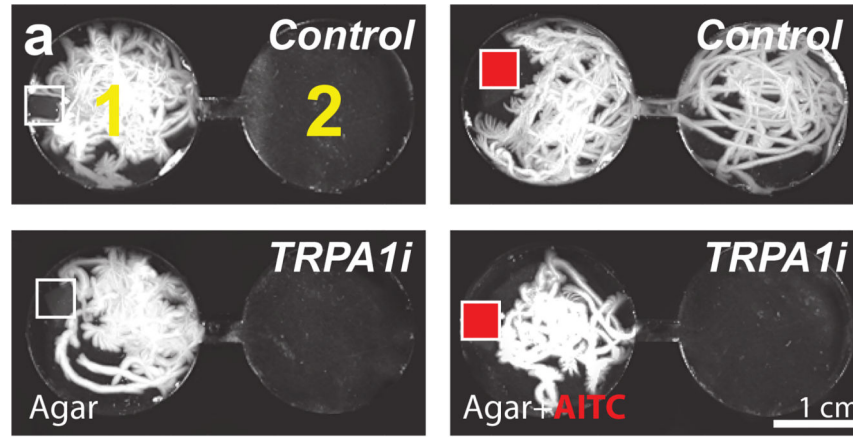


Figure 2. *Smed-TRPA1* is required for behavioral avoidance of the irritant chemical AITC. **a)** Two-chamber arena designed to quantify behavioral avoidance of chemical agonists of TRPA1. Planarian worms are introduced in chamber 1 in the presence of a mock Agar pellet (empty squares) or Agar+AITC (50 mM; red squares); their movement is then recorded for 5 minutes. The panels are maximum-projections of 5' movies, illustrating the extent of worm movement (white tracks). **b)** In the presence of agar alone, control (*unc22*), *ap2* and *Smed-TRPA1* RNAi worms do not readily cross the narrow channel connecting chambers 1 and 2. In the presence of AITC, both control (*unc22*) and *ap2* RNAi worms exit chamber 1 and

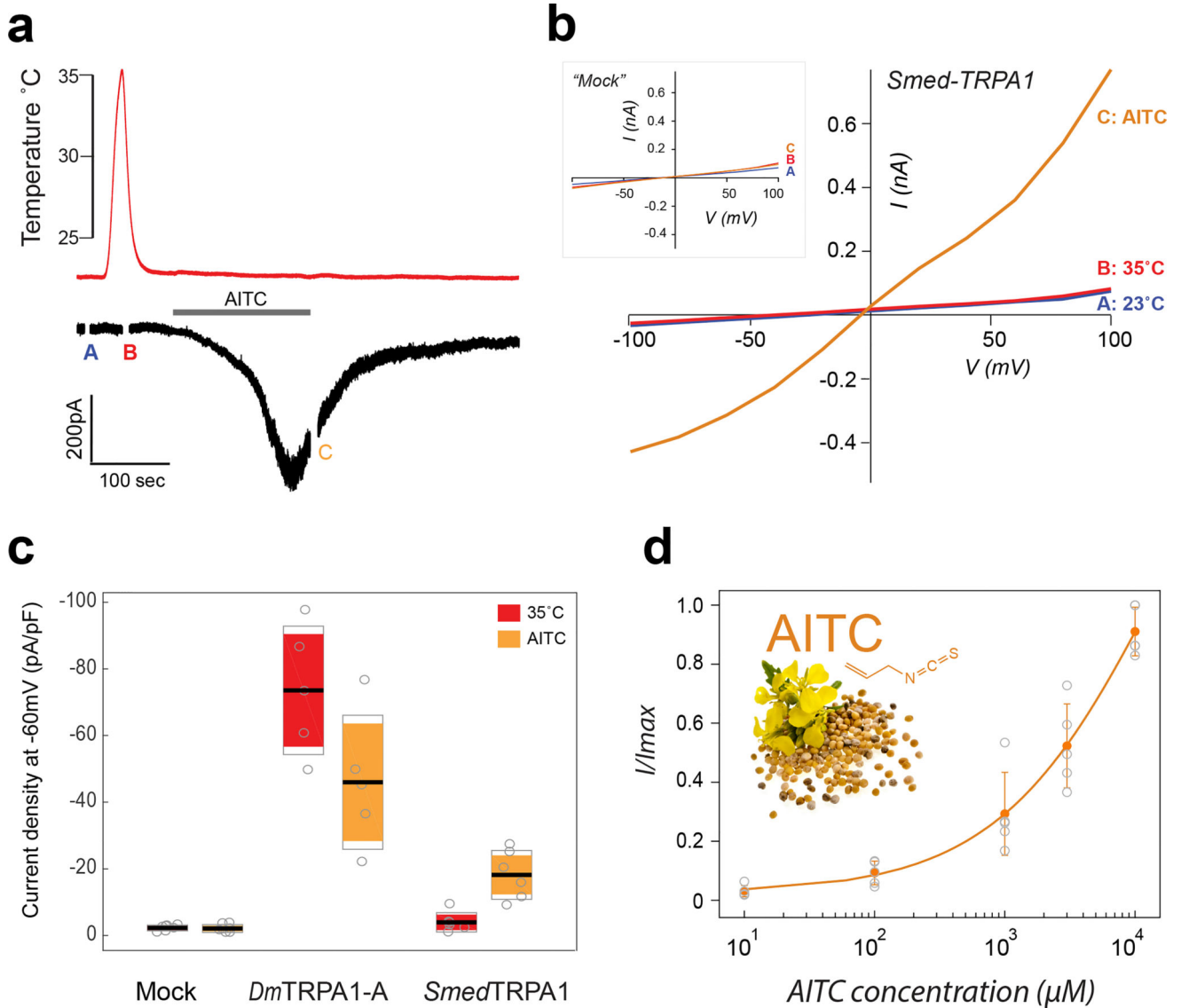
explore chamber 2. In contrast, *Smed-TRPA1* RNAi animals overwhelmingly remain in chamber 1 (N= 5 groups of 10 animals, fraction was calculated on the last 1' of video; *P=0.0078, Kruskal-Wallis comparing fraction of animals in chamber 1 or 2 across treatments; Chi-sq(2,12)=9.71; line=mean; outer boxes = +- STD; inner boxes = 95% Confidence Interval).

Author Manuscript

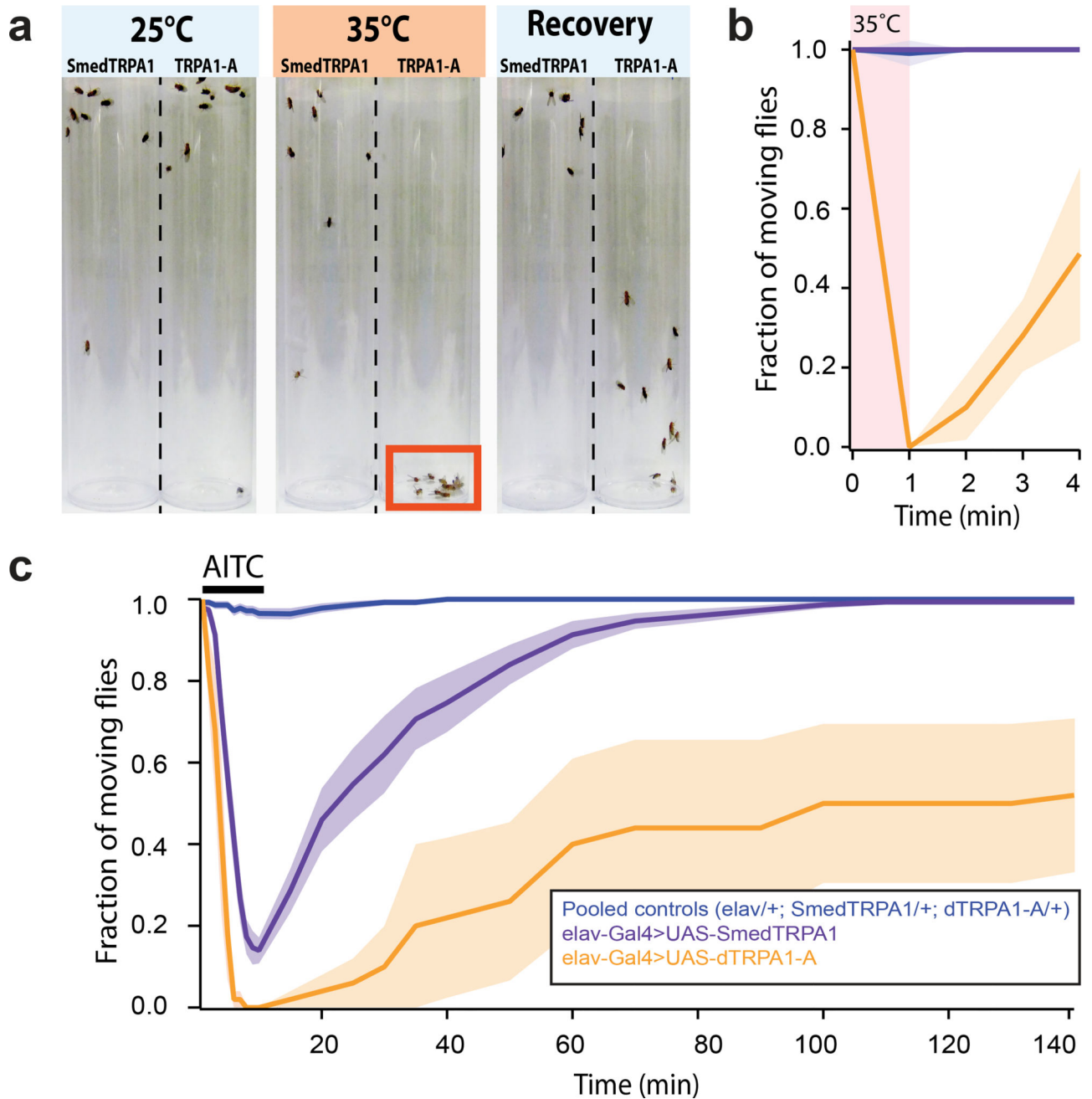
Author Manuscript

Author Manuscript

Author Manuscript

**Figure 3.**

Smed-TRPA1 expressed in *Drosophila* cells is activated by AITC but not by heat. **a**) S2R+ *Drosophila* cells voltage clamped at $-60mV$ were stimulated by heat (red trace) and by bath application of AITC ($500\mu M$, grey bar). AITC application (but not heating) resulted in an inward current. **b**) Current/Voltage relationship from averages of three step protocols done at room temperature (blue trace), during the heat stimulation (red trace), and at the end of AITC application (orange trace; note that the inset is a IV curve from a mock transfected cell; the timing of each set of measurements is also labeled as **A**, **B** and **C** on the trace shown in panel A). **c**) Current density (Max/capacitance) at $32^\circ C$ and in the presence of AITC recorded in mock-transfected, *dTRPA1-A* transfected, and *Smed-TRPA1* transfected cells. line=mean; outer boxes = \pm STD; inner boxes = 95% Confidence Interval. **d**). Dose-response for AITC activation of *Smed TRPA1* ($AV \pm$ STD; $n=5$ cells/condition; mustard flower and seed represent an iconic source of AITC).

**Figure 4.**

Functional expression of Smed-TRPA1 *in vivo* in adult *Drosophila* further demonstrates that the channel is sensitive to AITC but not to heat ($^{\circ}\text{C}$). **a**) Adult fruit flies expressing either Smed-TRPA1 or –as a control– the intrinsically heat sensitive *Drosophila* TRPA1-A splice variant, throughout the nervous system (under the control of elav-Gal4) were subjected to a brief step at 35 $^{\circ}\text{C}$ (a temperature which does not normally impair fly activity). TRPA1-A expressing flies are readily and reversibly incapacitated by heat (presumably because of simultaneous depolarization of neurons, caused by channel opening) and fall to the bottom of the tube; Smed-TRPA1 flies appear instead unaffected. **b**) Quantification of the

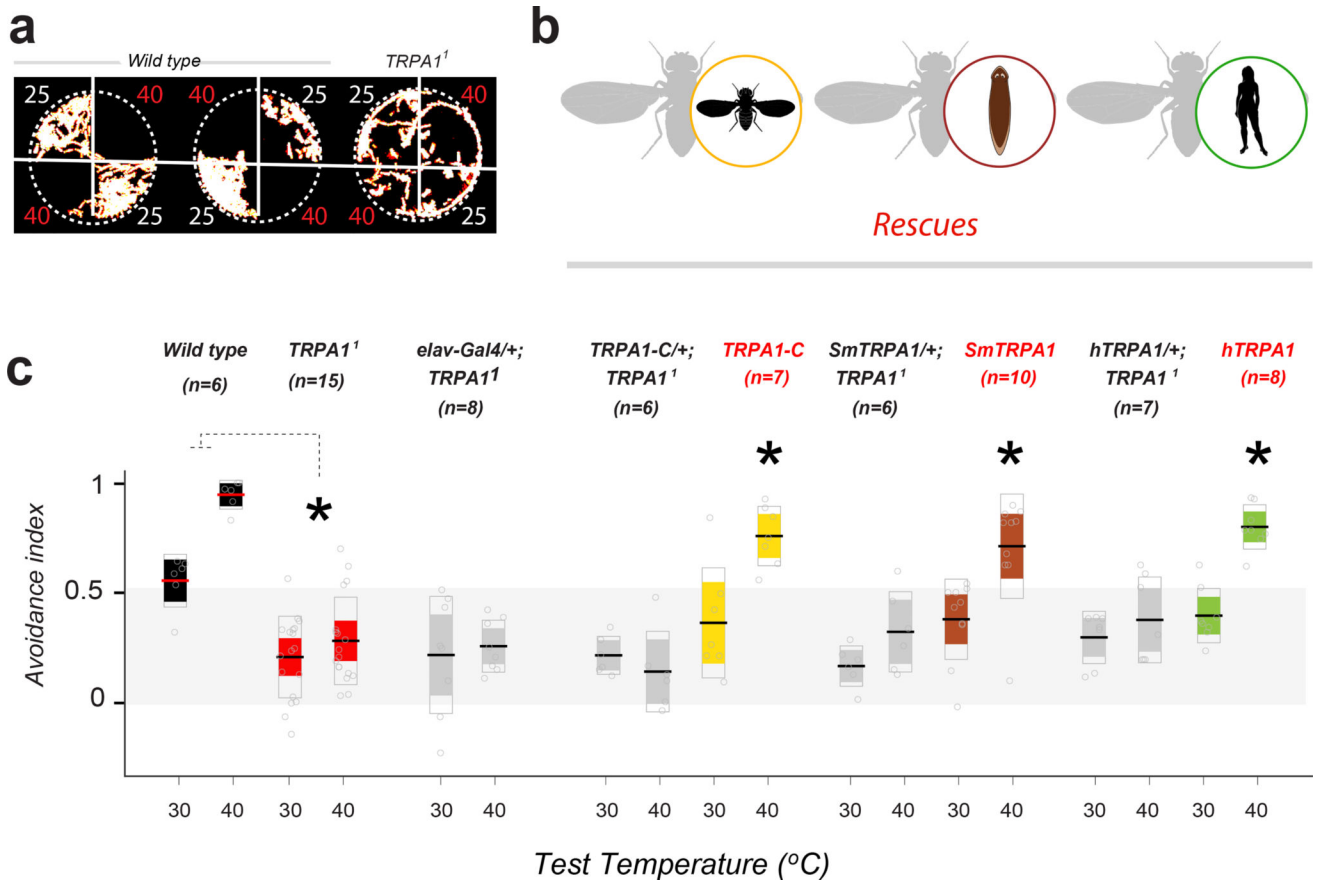
experiment in **a**. Blue trace = pooled controls (*elav/+; UAS-Smed-TRPA1/+; UAS-TRPA1-A/+*; N=4 groups of 10 animals for each, tested separately); purple trace = experimental animals (*elav-Gal4>UAS-Smed-TRPA1*; N=4 groups of 10 animals); orange trace = positive control (*elav-Gal4>UAS-TRPA1-A*; N=4 groups of 10 animals; for all traces shaded area \pm SEM). **c**) Adult flies expressing either Smed-TRPA1 or TRPA1-A were reversibly incapacitated by brief exposure to AITC vapors (see methods for details; Groups and Ns as above; shaded area \pm SEM).

Author Manuscript

Author Manuscript

Author Manuscript

Author Manuscript

**Figure 5.**

Across-phyllum rescue of *Drosophila* TRPA1 mutant phenotypes by planarian and human TRPA1. **a** In a 2-choice assay, wild type *Drosophila* flies robustly avoid noxious heat (40°C). In contrast, *TRPA1*¹ mutants explore more readily the 40°C quadrants (the panels are maximum-projections of 3' movies, illustrating the extent of fly movement, temperature in °C is indicated next to each quadrant). **b** Schematic of the rescue experiments. **c** Avoidance index of wild-type (black boxes), *TRPA1*¹ mutants (red), rescues (yellow, brown, green), and control genotypes (grey). *TRPA1*¹ mutants display a significantly lower avoidance index for heat (unpaired t-tests, 30°C: *P= 4.2 × e⁻⁴, t(19)=4.2578; 40°C: *P= 7.7 × e⁻⁷, t(19)=7.1991). Pan-neural expression (under the control of *elav-Gal4*) of mRNA encoding *Drosophila* TRPA1-C (a splice variant encoding a channel that is not heat-sensitive, yellow), *Smed-TRPA1* (brown), or human TRPA1 (green, each under a UAS-promoter) significantly rescues noxious heat avoidance (40°C). Control genotypes: *elav driver/+; TRPA1*¹ and UAS-transgene/+; *TRPA1*¹ (see methods for full genotypes). For rescues, AI values for each test temperature were compared by two-way ANOVAs; asterisks denote a significant interaction between the Gal4 and UAS transgene (from left: *P=0.0001, F(1,32)=19.32; *P=0.0092, F(1,35)=7.6; *P=0.0011, F(1,34)=12.7). Thick line = mean; outer boxes = +- STD; inner boxes = 95% Confidence Interval.

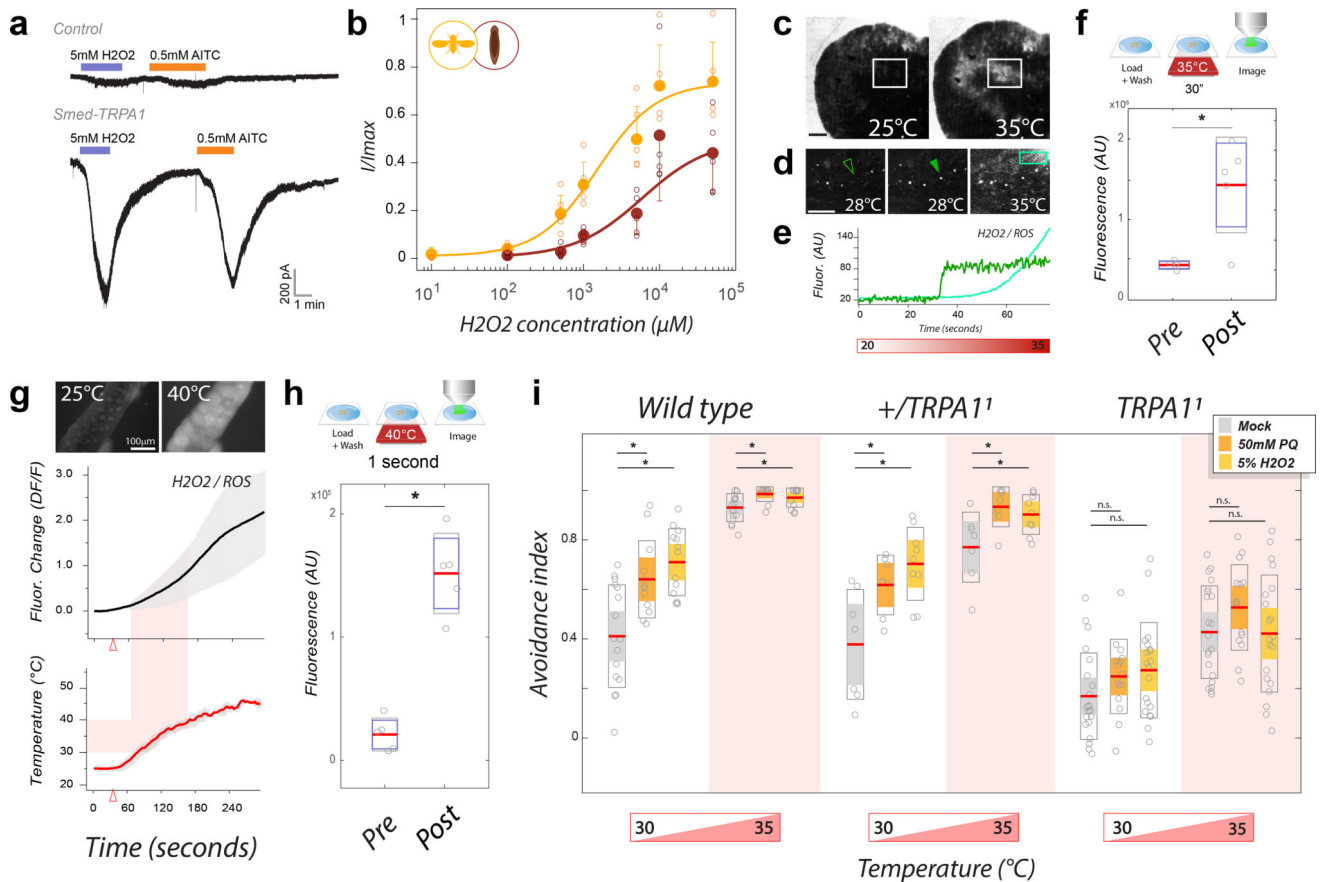


Figure 6.

$\text{H}_2\text{O}_2/\text{ROS}$ as a signal for TRPA1 activation during noxious heat responses. **a)** Heterologously expressed *Smed-TRPA1* is activated by H_2O_2 . **b)** Dose-response of H_2O_2 activation for *Drosophila* TRPA1-C (yellow trace and points), and *Smed-TRPA1* (brown trace and points, $\text{AV} \pm \text{STD}$, $n=5$ cells/condition). **c–e)** The ROS dye Carboxy- H_2DCFDA demonstrates *in vivo* ROS production in response to heat in living planarians. **c and d)** Representative frames of tissues and cells undergoing rapid fluorescent changes in response to heat (scale bar=200 μm). **e)** Traces are an ROI around the cell in **d** (arrow) and the square, light green box. **f)** Exposure of planarian worms to 35°C for 30" results in a significant increase in fluorescence (unpaired t-test, $*P=0.003$, $t(8)=4.1258$; $n=5$ /condition). **g)** Carboxy- H_2DCFDA fluorescence in response to heating in *Drosophila* salivary gland tissue ($\text{AV} \pm \text{SD}$). **h)** Exposure of salivary glands to 40°C for 1" results in a significant fluorescence increase (unpaired t-test, $*P=3.26 \times 10^{-5}$, $t(8)=8.3283$; $n=5$ /condition). **i)** Acute feeding with pro-oxidants sensitizes adult *Drosophila* to heat. Feeding Paraquat (orange bars) or H_2O_2 (yellow bars), results in increased heat avoidance in a 2-choice behavioral assay in both wild-type and heterozygous TRPA1/+ controls (unpaired t-tests; from left: $*P=0.003$, $t(26)=3.2093$, $n=16,12$; $*P=1.26 \times 10^{-4}$, $t(27)=4.472$, $n=16,13$; $*P=0.005$, $t(26)=3.058$, $n=16,12$; $*P=0.036$, $t(27)=2.201$, $n=16,13$; $*P=0.027$, $t(12)=-2.51$, $n=7,7$; $*P=0.003$, $t(14)=-3.53$, $n=7,9$; $*P=0.021$, $t(12)=-2.64$, $n=7,7$; $*P=0.033$, $t(14)=-2.35$, $n=7,9$). In contrast, heat avoidance does not increase in TRPA1 mutants (n.s. =not significant in unpaired t-tests; from left: $*P=0.16$, $t(34)=-1.43$, $n=21,15$; $*P=0.075$, $t(39)=-1.82$,

n=21,20; *P= 0.11, t(34)=-1.62, n=21,15; *P= 0.93, t(39)=0.088, n=21,20;. In **f**, **h** and **i**:
Line=mean; outer boxes = +- STD; inner boxes = 95% Confidence Interval).

Author Manuscript

Author Manuscript

Author Manuscript

Author Manuscript